

Supporting Information

A microporous lanthanum metal-organic framework as a bi-functional chemosensor for the detection of picric acid and Fe³⁺ ions

Chuanqi Zhang,^a Yan Yan,^a Qinhe Pan,^b Libo Sun,^a Hongming He,^a Yunling Liu,^a

Zhiqiang Liang*^a and Jiyang Li*^a

^a State Key Laboratory of Inorganic Synthesis and Preparative Chemistry, College of Chemistry, Jilin University, Changchun 130012, P. R. China

^b Department of Materials and Chemical Engineering, Hainan University, Haikou, 570228, P. R. China.

Table S1 Crystal Data and Structure Refinement for **1**.^a

Empirical formula	C ₂₅ H ₂₅ La O ₉ S ₂	
Formula weight	672.49	
Temperature	296(2) K	
Wavelength	0.71073 Å	
Crystal system, space group	Monoclinic, C2/c	
	<i>a</i> = 33.400(4) Å	α = 90°
Unit cell dimensions	<i>b</i> = 13.8787(19) Å	β = 104.966(3)°
	<i>c</i> = 13.5790(16) Å	γ = 90°
Volume	6081.0(13) Å ³	
Z	8	
Absorption coefficient	1.580 mm ⁻¹	
<i>F</i> (000)	2512	
Theta range for data collection	1.26 to 26.67°	
Limiting indices	-28 ≤ <i>h</i> ≤ 41, -17 ≤ <i>k</i> ≤ 17, -16 ≤ <i>l</i> ≤ 16	
Reflections collected / unique	21624 / 6316	
<i>R</i> _{int}	0.0778	
Completeness to theta = 28.21	98.3 %	
Absorption correction	Semi-empirical from equivalents	
Max. and min. transmission	0.8209 and 0.7640	
Refinement method	Full-matrix least-squares on <i>F</i> ²	
Data / restraints / parameters	6316 / 90 / 332	
Goodness-of-fit on <i>F</i> ²	1.006	
Final R indices [<i>I</i> >2σ(<i>I</i>)] ^b	<i>R</i> ₁ = 0.0583, <i>wR</i> ₂ = 0.1562	
<i>R</i> indices (all data)	<i>R</i> ₁ = 0.0748, <i>wR</i> ₂ = 0.1665	
Largest diff. peak and hole	2.526 and -2.250 e. Å ⁻³	

^aDate based on PLATON/SQUEEZE mode.^b $R_1 = \sum |F_o| - |F_c| / \sum |F_o|$. $wR_2 = [\sum [w(F_o^2 - F_c^2)^2] / \sum [w(F_o^2)^2]]^{1/2}$.

Table S2 Selected bond lengths [Å] and angles [°] for **1**.

Bond lengths		Bond lengths	
La(1)-O(3)#1	2.482(2)	C(6)-H(6)	0.93
La(1)-O(8)	2.495(2)	C(7)-C(8)	1.3984
La(1)-O(7)	2.503(2)	C(7)-C(12)	1.4129
La(1)-O(2)	2.505(2)	C(8)-C(9)	1.3836
La(1)-O(1)	2.512(2)	C(8)-H(8)	0.93
La(1)-O(6)	2.555(2)	C(9)-C(10)	1.4009
La(1)-O(4)	2.563(2)	C(9)-H(9)	0.93
La(1)-O(5)	2.596(2)	C(10)-C(11)	1.3876
La(1)-O(3)	2.7756(18)	C(10)-C(13)	1.483
La(1)-C(21)	2.931(3)	C(11)-C(12)	1.4045
La(1)-C(20)	3.036(3)	C(11)-H(11)	0.93
La(1)-La(1)#1	4.1812(5)	C(12)-H(12)	0.93
O(1)-C(19)	1.254(4)	C(13)-C(14)	1.3865
O(2)-C(19)#1	1.253(4)	C(13)-C(18)	1.4156
O(3)-C(20)	1.267(3)	C(14)-C(15)	1.3978
O(3)-La(1)#1	2.482(2)	C(14)-H(14)	0.93
O(4)-C(20)	1.242(3)	C(15)-C(16)	1.3963
O(5)-C(21)	1.249(4)	C(15)-C(19)	1.506(3)
O(6)-C(21)	1.267(4)	C(16)-C(17)	1.385
O(7)-S(1)	1.475(3)	C(16)-H(16)	0.93
O(7)-S(1')	1.523(6)	C(17)-C(18)	1.4003
O(8)-S(2)	1.415(3)	C(17)-C(20)#3	1.507(3)
O(8)-S(2')	1.604(5)	C(18)-H(18)	0.93
C(1)-C(2)	1.39	C(19)-O(2)#1	1.253(4)
C(1)-C(6)	1.39	C(20)-C(17)#4	1.507(4)
C(1)-C(21)#2	1.508(3)	C(21)-C(1)#5	1.508(3)
C(2)-C(3)	1.39	C(22)-S(1)	1.510(7)
C(2)-H(2)	0.93	C(22')-S(1')	1.472(12)
C(3)-C(4)	1.39	S(1)-C(23)	1.562(9)
C(3)-H(3)	0.93	S(1')-C(23')	1.556(13)
C(4)-C(5)	1.39	S(2)-C(24)	1.546(7)
C(4)-C(7)	1.5028	S(2)-C(25)	1.641(8)
C(5)-C(6)	1.39	S(2')-C(24')	1.544(8)
C(5)-H(5)	0.93	S(2')-C(25')	1.618(13)

Bond angles		Bond angels	
O(3)#1-La(1)-O(8)	82.56(8)	C(2)-C(1)-C(21)#2	119.95(14)
O(3)#1-La(1)-O(7)	149.35(8)	C(6)-C(1)-C(21)#2	119.98(14)
O(8)-La(1)-O(7)	76.47(9)	C(3)-C(2)-C(1)	120
O(3)#1-La(1)-O(2)	72.46(7)	C(3)-C(2)-H(2)	120
O(8)-La(1)-O(2)	137.03(8)	C(1)-C(2)-H(2)	120
O(7)-La(1)-O(2)	137.35(8)	C(2)-C(3)-C(4)	120
O(3)#1-La(1)-O(1)	79.13(7)	C(2)-C(3)-H(3)	120
O(8)-La(1)-O(1)	74.01(9)	C(4)-C(3)-H(3)	120
O(7)-La(1)-O(1)	73.79(8)	C(5)-C(4)-C(3)	120
O(2)-La(1)-O(1)	131.61(6)	C(5)-C(4)-C(7)	120.6
O(3)#1-La(1)-O(6)	132.83(7)	C(3)-C(4)-C(7)	119.4
O(8)-La(1)-O(6)	94.50(9)	C(6)-C(5)-C(4)	120
O(7)-La(1)-O(6)	71.63(9)	C(6)-C(5)-H(5)	120
O(2)-La(1)-O(6)	78.88(7)	C(4)-C(5)-H(5)	120
O(1)-La(1)-O(6)	145.24(7)	C(5)-C(6)-C(1)	120
O(3)#1-La(1)-O(4)	120.68(6)	C(5)-C(6)-H(6)	120
O(8)-La(1)-O(4)	149.47(8)	C(1)-C(6)-H(6)	120
O(7)-La(1)-O(4)	74.03(8)	C(8)-C(7)-C(12)	117.2
O(2)-La(1)-O(4)	72.65(7)	C(8)-C(7)-C(4)	122.1
O(1)-La(1)-O(4)	90.28(8)	C(12)-C(7)-C(4)	120.7
O(6)-La(1)-O(4)	83.59(7)	C(9)-C(8)-C(7)	121.7
O(3)#1-La(1)-O(5)	84.25(7)	C(9)-C(8)-H(8)	119.1
O(8)-La(1)-O(5)	72.62(9)	C(7)-C(8)-H(8)	119.1
O(7)-La(1)-O(5)	109.89(8)	C(8)-C(9)-C(10)	120.7
O(2)-La(1)-O(5)	70.60(7)	C(8)-C(9)-H(9)	119.6
O(1)-La(1)-O(5)	144.27(7)	C(10)-C(9)-H(9)	119.6
O(6)-La(1)-O(5)	50.72(7)	C(11)-C(10)-C(9)	118.8
O(4)-La(1)-O(5)	125.30(7)	C(11)-C(10)-C(13)	122
O(3)#1-La(1)-O(3)	74.77(7)	C(9)-C(10)-C(13)	119.1
O(8)-La(1)-O(3)	136.84(9)	C(10)-C(11)-C(12)	120.3
O(7)-La(1)-O(3)	106.13(7)	C(10)-C(11)-H(11)	119.8
O(2)-La(1)-O(3)	69.12(6)	C(12)-C(11)-H(11)	119.8
O(1)-La(1)-O(3)	66.03(6)	C(11)-C(12)-C(7)	121
O(6)-La(1)-O(3)	127.77(7)	C(11)-C(12)-H(12)	119.5
O(4)-La(1)-O(3)	48.40(6)	C(7)-C(12)-H(12)	119.5
O(5)-La(1)-O(3)	138.54(6)	C(14)-C(13)-C(18)	118.7
O(3)#1-La(1)-C(21)	108.28(8)	C(14)-C(13)-C(10)	121.4
O(8)-La(1)-C(21)	83.72(10)	C(18)-C(13)-C(10)	119.9
O(7)-La(1)-C(21)	91.51(9)	C(13)-C(14)-C(15)	121.9
O(2)-La(1)-C(21)	72.20(8)	C(13)-C(14)-H(14)	119

O(1)-La(1)-C(21)	155.54(7)	C(15)-C(14)-H(14)	119
O(6)-La(1)-C(21)	25.56(9)	C(16)-C(15)-C(14)	119
O(4)-La(1)-C(21)	104.61(8)	C(16)-C(15)-C(19)	119.71(12)
O(5)-La(1)-C(21)	25.19(8)	C(14)-C(15)-C(19)	121.20(12)
O(3)-La(1)-C(21)	138.08(7)	C(17)-C(16)-C(15)	119.7
O(3)#1-La(1)-C(20)	98.11(7)	C(17)-C(16)-H(16)	120.1
O(8)-La(1)-C(20)	151.23(9)	C(15)-C(16)-H(16)	120.1
O(7)-La(1)-C(20)	90.08(8)	C(16)-C(17)-C(18)	121.4
O(2)-La(1)-C(20)	68.60(7)	C(16)-C(17)-C(20)#3	118.93(12)
O(1)-La(1)-C(20)	77.87(8)	C(18)-C(17)-C(20)#3	119.69(12)
O(6)-La(1)-C(20)	105.36(8)	C(17)-C(18)-C(13)	119
O(4)-La(1)-C(20)	23.75(7)	C(17)-C(18)-H(18)	120.5
O(5)-La(1)-C(20)	136.15(7)	C(13)-C(18)-H(18)	120.5
O(3)-La(1)-C(20)	24.66(7)	O(2)#1-C(19)-O(1)	126.0(3)
C(21)-La(1)-C(20)	122.49(9)	O(2)#1-C(19)-C(15)	117.0(2)
O(3)#1-La(1)-La(1)#1	39.83(4)	O(1)-C(19)-C(15)	117.0(2)
O(8)-La(1)-La(1)#1	114.03(7)	O(4)-C(20)-O(3)	122.3(2)
O(7)-La(1)-La(1)#1	134.03(7)	O(4)-C(20)-C(17)#4	118.3(2)
O(2)-La(1)-La(1)#1	65.45(5)	O(3)-C(20)-C(17)#4	119.4(2)
O(1)-La(1)-La(1)#1	67.57(4)	O(4)-C(20)-La(1)	56.23(14)
O(6)-La(1)-La(1)#1	144.10(5)	O(3)-C(20)-La(1)	66.06(14)
O(4)-La(1)-La(1)#1	82.08(4)	C(17)#4-C(20)-La(1)	173.88(18)
O(5)-La(1)-La(1)#1	115.98(5)	O(5)-C(21)-O(6)	122.6(3)
O(3)-La(1)-La(1)#1	34.94(4)	O(5)-C(21)-C(1)#5	119.3(3)
C(21)-La(1)-La(1)#1	132.85(6)	O(6)-C(21)-C(1)#5	118.1(3)
C(20)-La(1)-La(1)#1	58.70(5)	O(5)-C(21)-La(1)	62.23(17)
C(19)-O(1)-La(1)	135.56(19)	O(6)-C(21)-La(1)	60.44(16)
C(19)#1-O(2)-La(1)	134.2(2)	C(1)#5-C(21)-La(1)	175.04(18)
C(20)-O(3)-La(1)#1	156.01(17)	O(7)-S(1)-C(22)	92.4(3)
C(20)-O(3)-La(1)	89.28(15)	O(7)-S(1)-C(23)	120.8(5)
La(1)#1-O(3)-La(1)	105.23(7)	C(22)-S(1)-C(23)	95.0(5)
C(20)-O(4)-La(1)	100.03(18)	C(22')-S(1')-O(7)	118.2(6)
C(21)-O(5)-La(1)	92.6(2)	C(22')-S(1')-C(23')	117.8(11)
C(21)-O(6)-La(1)	94.00(19)	O(7)-S(1')-C(23')	105.1(10)
S(1)-O(7)-S(1')	56.1(2)	O(8)-S(2)-C(24)	113.9(5)
S(1)-O(7)-La(1)	137.61(18)	O(8)-S(2)-C(25)	113.3(4)
S(1')-O(7)-La(1)	141.7(2)	C(24)-S(2)-C(25)	93.6(6)
S(2)-O(8)-S(2')	40.9(2)	C(24')-S(2')-O(8)	114.1(5)
S(2)-O(8)-La(1)	146.9(2)	C(24')-S(2')-C(25')	98.3(9)
S(2')-O(8)-La(1)	127.9(2)	O(8)-S(2')-C(25')	84.3(10)
C(2)-C(1)-C(6)	120		

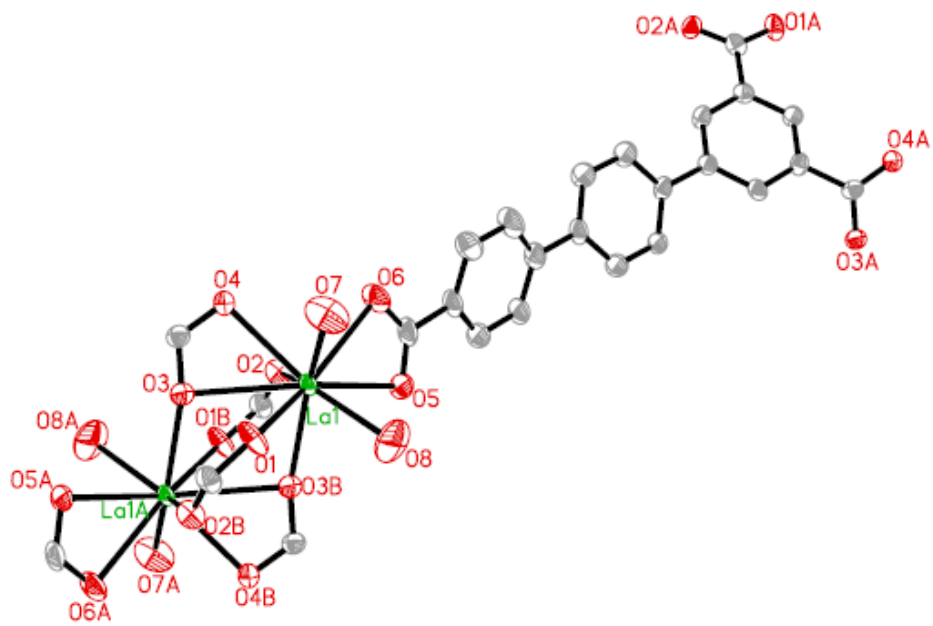


Fig. S1 The asymmetric unit of **1** showing ellipsoid at the 50% probability level.

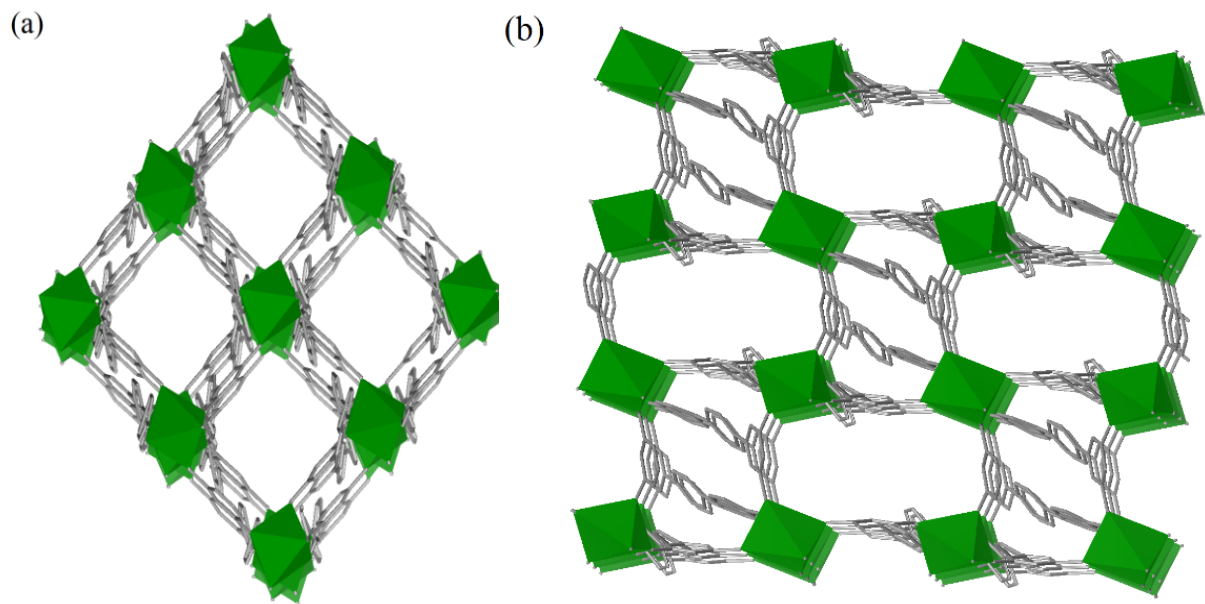


Fig. S2 Framework structure of **1** showing the channels along a) [-101] and b) [110] direction, respectively. The bi-nuclear $\text{La}_2(\text{COO})_6$ clusters are simplified into octahedral polyhedrons. Hydrogen atoms, terminal DMSO molecules, and free H_2O molecules are omitted for charity.

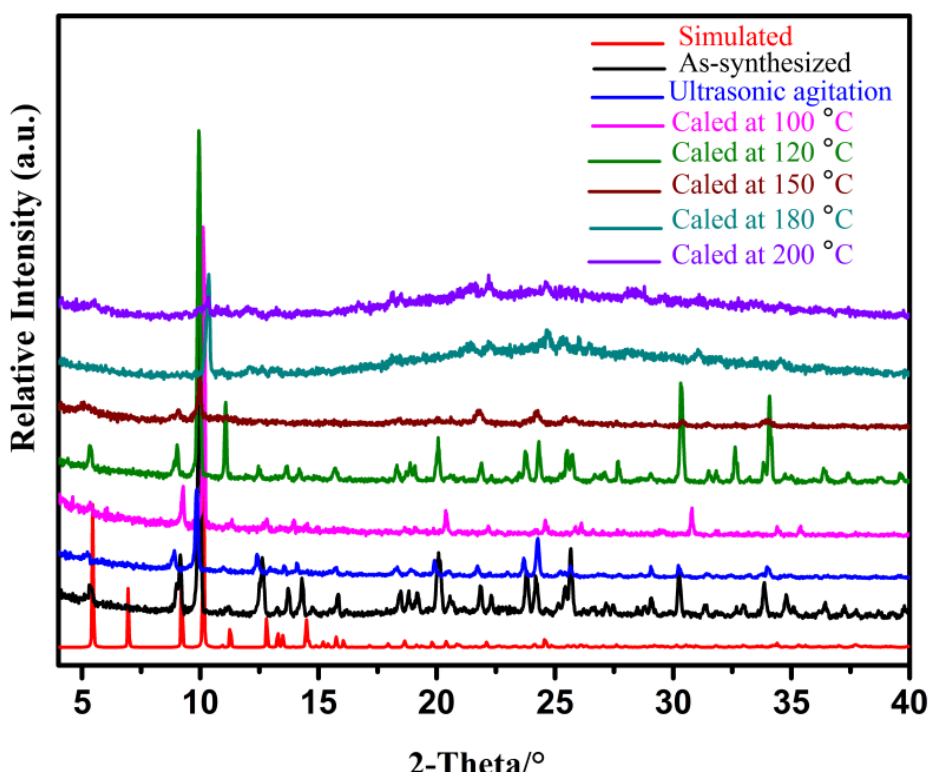


Fig. S3 The PXRD patterns of **1** at different temperatures and after ultrasonic agitation, the simulated one calculated from the single crystal structure analysis.

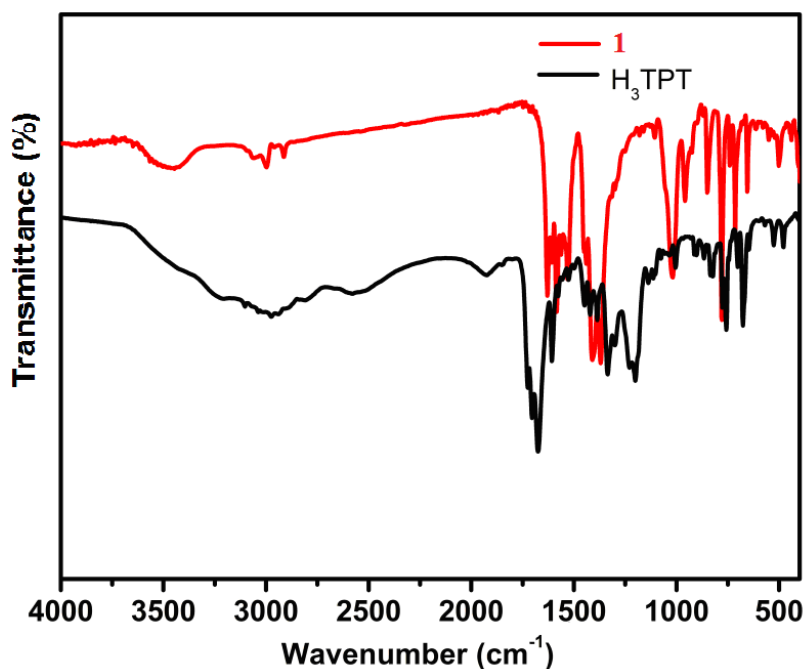


Fig. S4 IR spectra of H₃TPT and **1**.

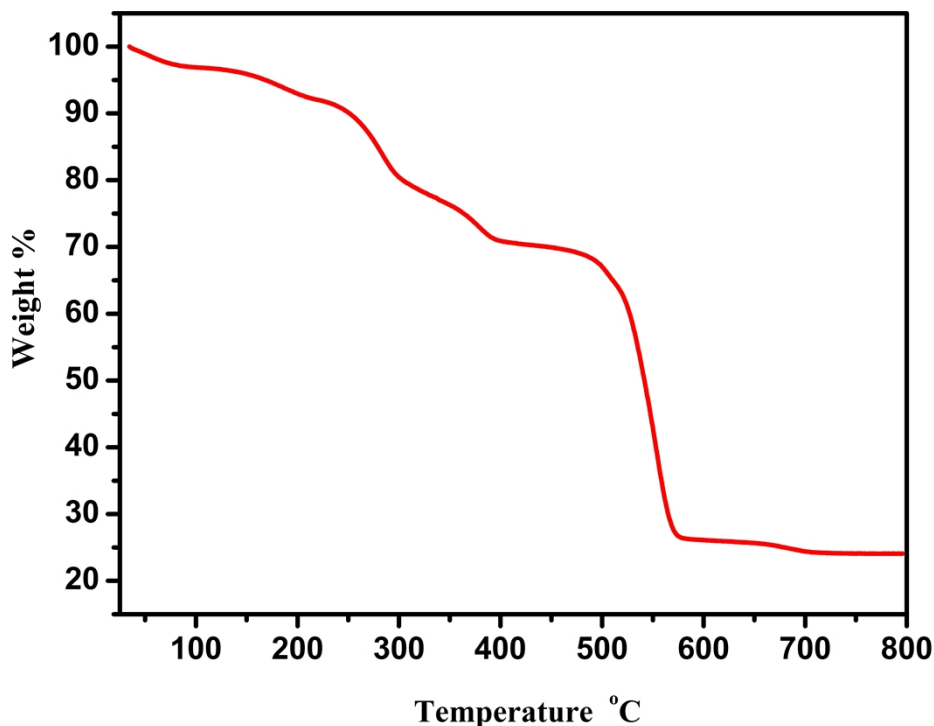


Fig. S5 TGA curve of **1**

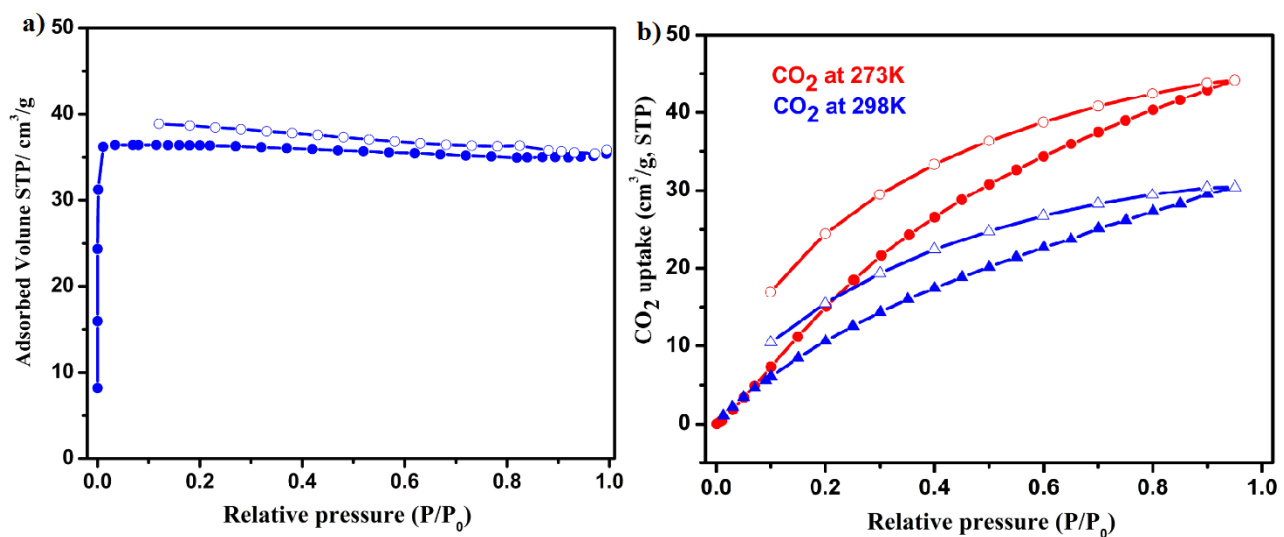


Fig. S6 a) N₂ adsorption-desorption isotherms of **1** at 77 K. b) CO₂ adsorption-desorption isotherms of **1** at 273 K and 298 K.

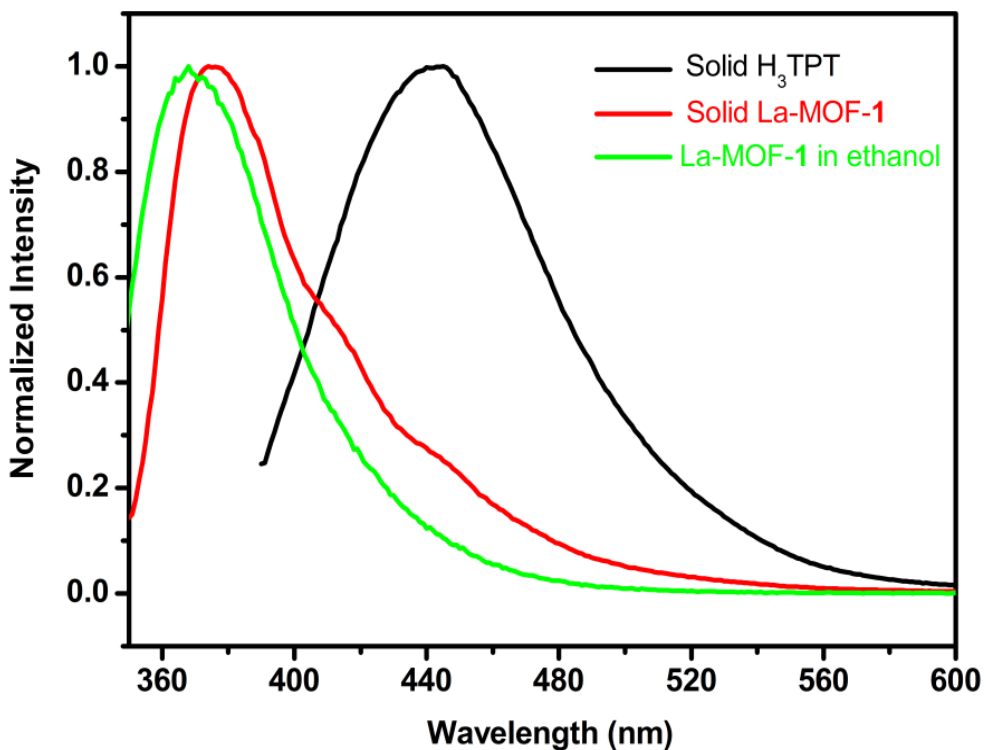


Fig. S7 Emission spectra of H₃TPT ligand ($\lambda_{\text{ex}} = 370$ nm) and **1** ($\lambda_{\text{ex}} = 342$ nm) in solid state, as well as **1** dispersed in ethanol.

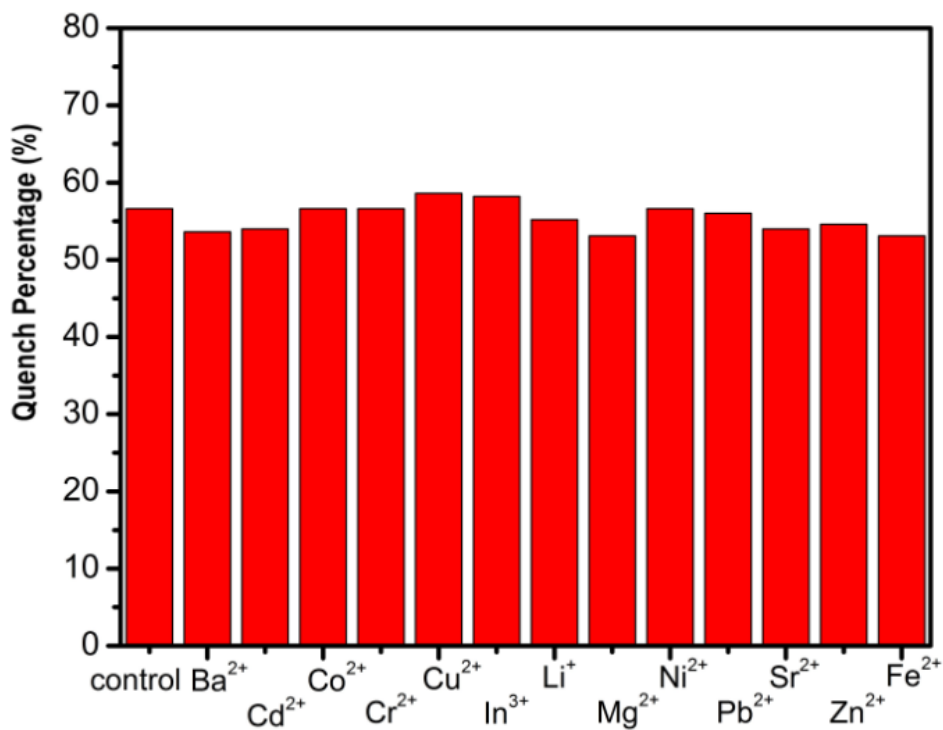


Fig. S8 Effects of the coexisting metal ions with the same amount of Fe³⁺ ions on the quenched fluorescent intensity of **1**-ethanol suspension by Fe³⁺ ions (Fe³⁺ ions with the concentration of 95.2 μM is taken as control).

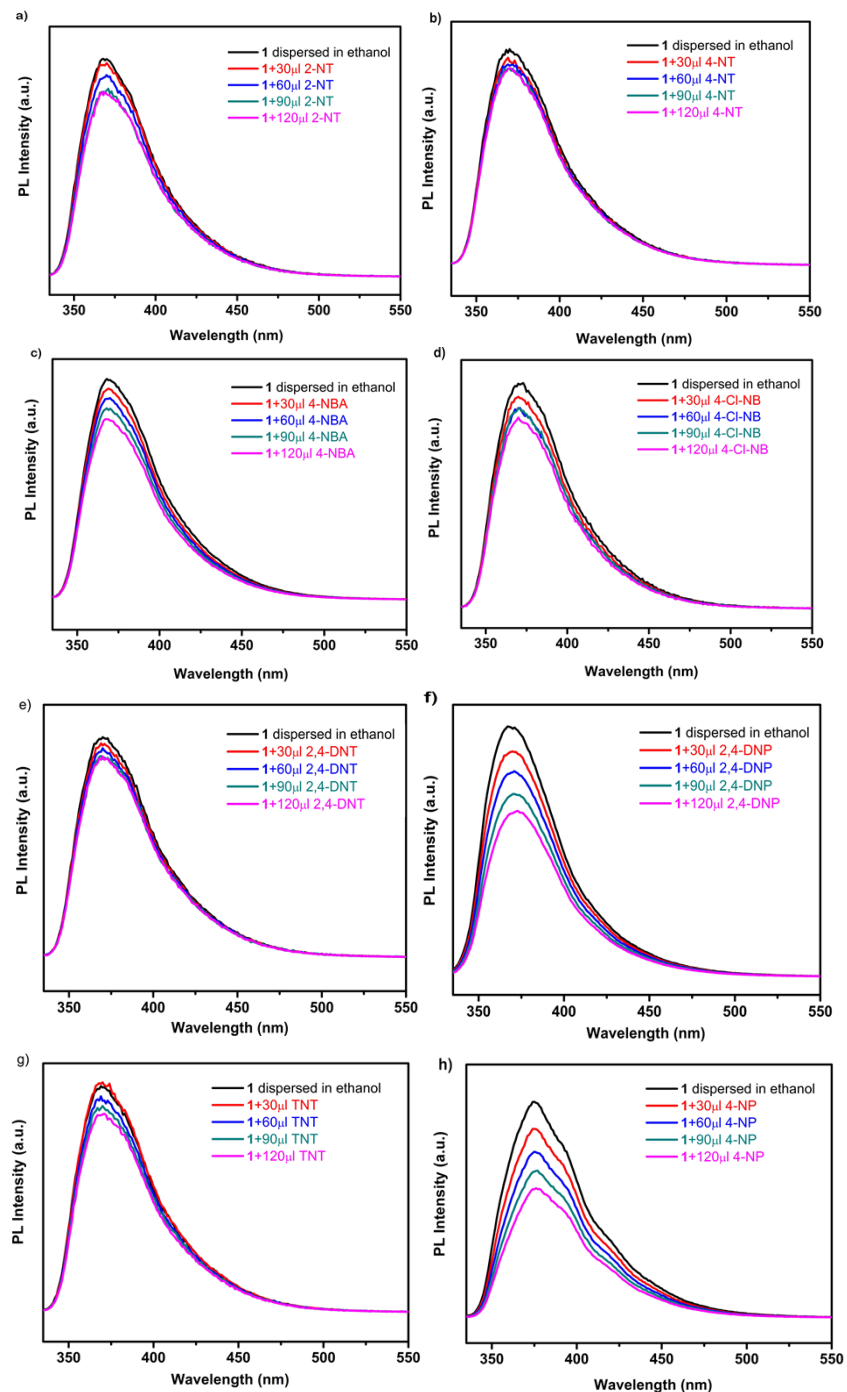


Fig. S9 Fluorescent titrations of 0.5mg **1** dispersed in 2mL ethanol solution with the addition of different volume of 0.001M solution of a) 2-nitrotoluene (2-NT), b) 4-nitrotoluene (4-NT), c) 4-nitrobenzaldehyde (4-NBA), d) 4-chloronitrobenzene (4-Cl-NB), e) 2, 4-di nitrotoluene (2,4-DNT), f) 2, 4-dinitrophenol (2,4-DNP), g) 2, 4, 6-trinitrotoluene (TNT), and h) 4-nitrophenol (4-NP) in ethanol. The fluorescent emission spectra were recorded from 350 nm to 550 nm upon the excitation at 329nm. The slit width for excitation and emission is 5.0 nm and 3.0 nm, respectively.

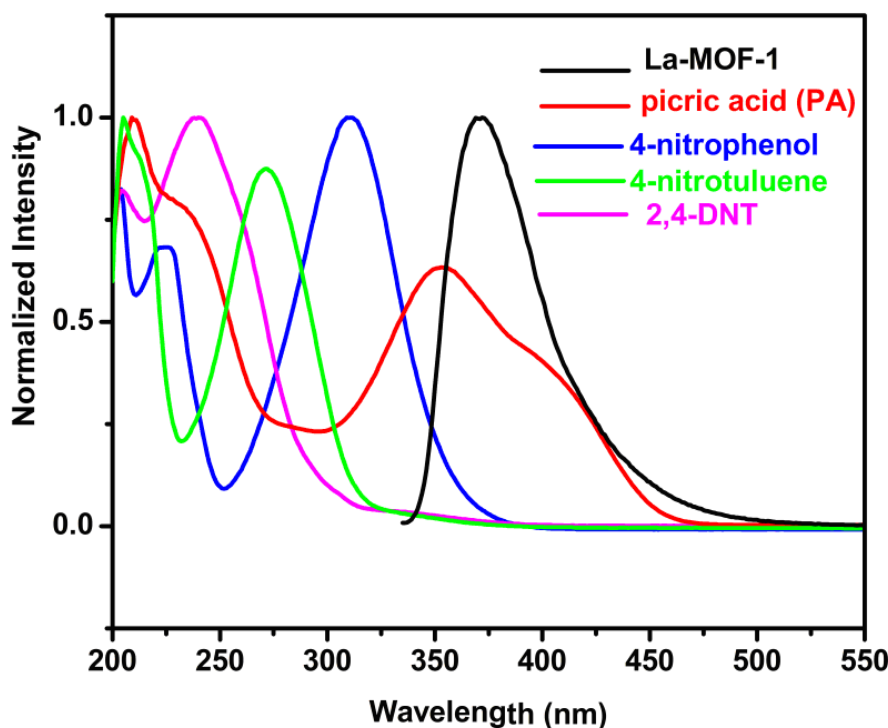


Fig. S10 Spectral overlaps between the absorption spectra of analytes with the concentration of 1.0×10^{-3} M and the emission spectra of **1** in ethanol.

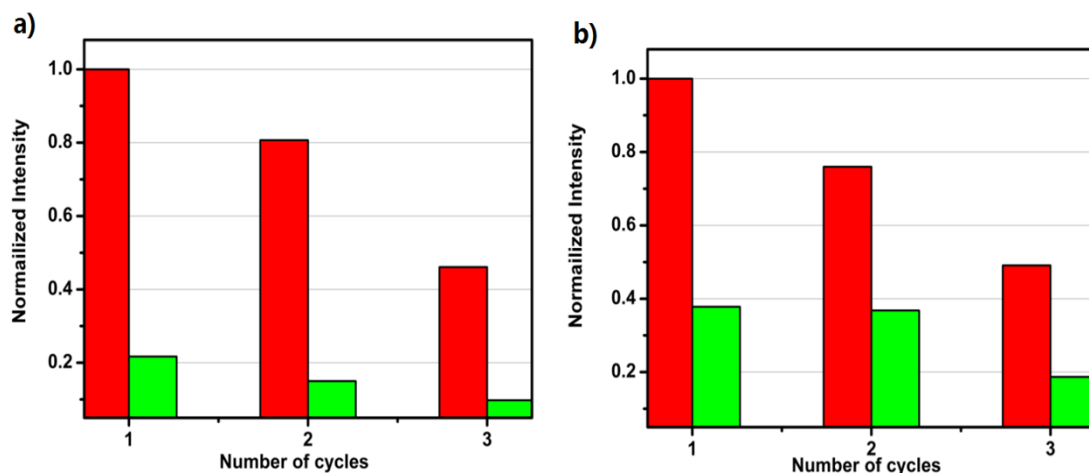


Fig. S11 The quenching and recovery test of **1** for a) PA and b) Fe^{3+} ions, respectively. red : the original fluorescence intensity; green : the intensity upon addition of PA and Fe^{3+} ions.

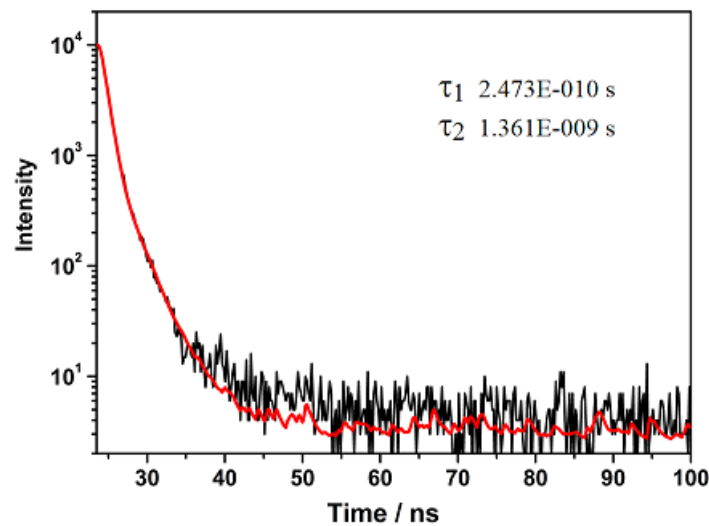


Fig. S12 Time-dependent fluorescence decay data of **1** monitored at 366 nm at room temperature. The black line and the red line represent the experimental data and the best fits of experimental data, respectively.